

AD-A167 939

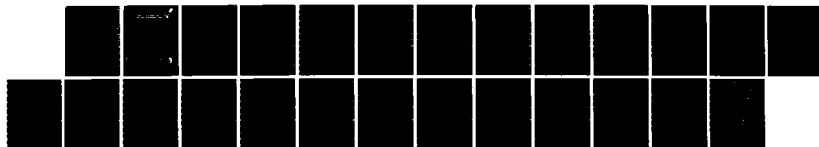
EVALUATION OF FULL-SCALE HOVERCRAFT LIFT SYSTEMS(U)
DAVID M TAYLOR NAVAL SHIP RESEARCH AND DEVELOPMENT
CENTER BETHESDA MD D D MORAN ET AL. MAR 86
DTNSRDC-86/016

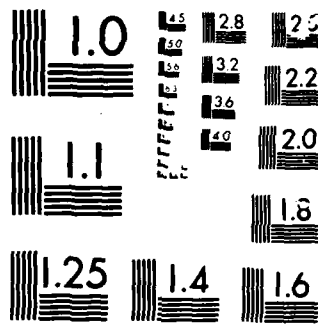
1/1

UNCLASSIFIED

F/G 1/3

NL





MICROCOPY

CHART

DTNSRDC-86/016

AD-A167 939

EVALUATION OF FULL-SCALE HOVERCRAFT LIFT SYSTEMS

DAVID W. TAYLOR NAVAL SHIP RESEARCH AND DEVELOPMENT CENTER

Bethesda, Maryland 20884-5000



EVALUATION OF FULL-SCALE HOVERCRAFT LIFT SYSTEMS

by

David D. Moran
R. Thomas Waters

and

Alan N. Jennings
Technology Applications
Engineering Services Group
Falls Church, Virginia

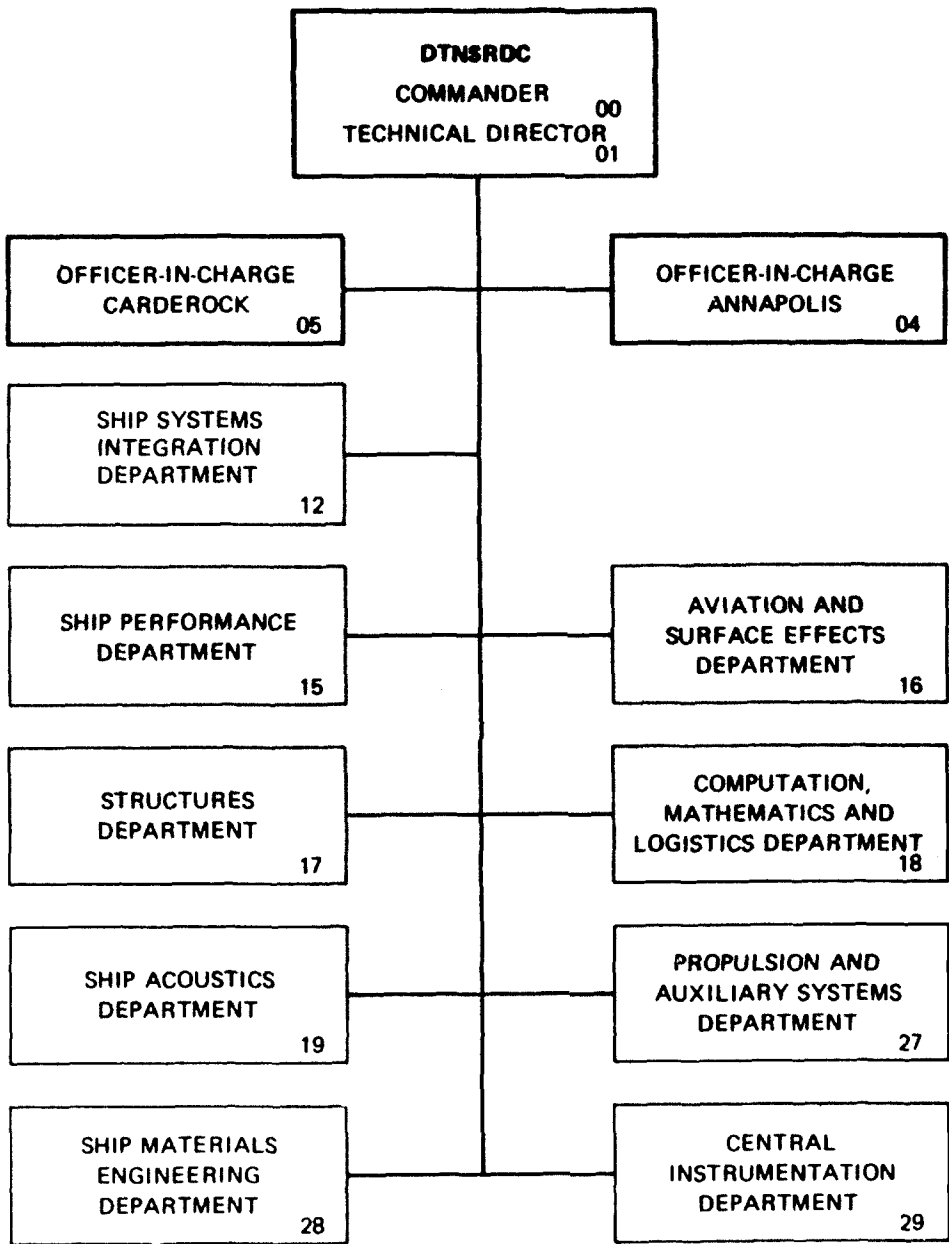
APPROVED FOR PUBLIC RELEASE; DISTRIBUTION IS UNLIMITED.

OFFICE OF DIRECTOR OF TECHNOLOGY
RESEARCH AND DEVELOPMENT REPORT

March 1986

DTNSRDC-86/016

MAJOR DTNSRDC ORGANIZATIONAL COMPONENTS



UNCLASSIFIED

SECURITY CLASSIFICATION OF THIS PAGE

AD-A167939

REPORT DOCUMENTATION PAGE

1a. REPORT SECURITY CLASSIFICATION UNCLASSIFIED		1b. RESTRICTIVE MARKINGS	
2a. SECURITY CLASSIFICATION AUTHORITY		3. DISTRIBUTION / AVAILABILITY OF REPORT APPROVED FOR PUBLIC RELEASE; DISTRIBUTION IS UNLIMITED.	
2b. DECLASSIFICATION / DOWNGRADING SCHEDULE		4. PERFORMING ORGANIZATION REPORT NUMBER(S) DTNSRDC-86/016	
6a. NAME OF PERFORMING ORGANIZATION David W. Taylor Naval Ship R&D Center		6b. OFFICE SYMBOL (If applicable) Code 012.3	
7a. NAME OF MONITORING ORGANIZATION Amphibious Assault Landing Craft Office DTNSRDC, Code 1232		7b. ADDRESS (City, State, and ZIP Code) Bethesda, Maryland 20084-5000	
8a. NAME OF FUNDING / SPONSORING ORGANIZATION		8b. OFFICE SYMBOL (If applicable)	
9. PROCUREMENT INSTRUMENT IDENTIFICATION NUMBER		10. SOURCE OF FUNDING NUMBERS	
8c. ADDRESS (City, State, and ZIP Code)		PROGRAM ELEMENT NO	PROJECT NO
		TASK NO 14174	WORK UNIT ACCESSION NO
11. TITLE (Include Security Classification) EVALUATION OF FULL-SCALE HOVERCRAFT LIFT SYSTEMS			
12. PERSONAL AUTHOR(S) Moran, D.D., DTNSRDC; Waters, R. Thomas, DTNSRDC; and (Continued on reverse side)			
13a. TYPE OF REPORT Final	13b. TIME COVERED FROM TO	14. DATE OF REPORT (Year, Month, Day) 1986, March	15. PAGE COUNT 21
16. SUPPLEMENTARY NOTATION			
17. COSATI CODES		18. SUBJECT TERMS (Continue on reverse if necessary and identify by block number)	
FIELD	GROUP	SUB-GROUP	
		Hovercraft, lift systems, ACV, ACV cushion, ACV lift system, ACV fans	
19. ABSTRACT (Continue on reverse if necessary and identify by block number)			
<p>The design of a hovercraft lift system is normally based upon fairly simple hydraulic models of the lift system components. Lift system loss coefficients and fan efficiencies are determined from prior experience, empirical data bases and components or system model studies. The prediction of full-scale performance is complicated by the difficulty of establishing correspondence between model-scale and full-scale values of Reynolds number, Mach number and Euler number. Full-scale verification of the lift system design process is an essential part of hovercraft development.</p> <p>This paper presents the results of a full-scale evaluation of the performance of a hovercraft lift system, and performance characteristics are compared with model-scale results. Comparisons of lift system loss coefficients show good correlation, but lift system efficiencies are shown to be significantly higher in full-scale results than from</p> <p>(Continued on the reverse side)</p>			
20. DISTRIBUTION / AVAILABILITY OF ABSTRACT <input checked="" type="checkbox"/> UNCLASSIFIED UNLIMITED <input type="checkbox"/> SAME AS RPT <input type="checkbox"/> DTIC USERS		21. ABSTRACT SECURITY CLASSIFICATION UNCLASSIFIED	
22a. NAME OF RESPONSIBLE INDIVIDUAL David D. Moran		22b. TELEPHONE (Include Area Code) (202) 227-1275	22c. OFFICE SYMBOL Code 012.3

UNCLASSIFIED

SECURITY CLASSIFICATION OF THIS PAGE

(Block 12 continued)

Jennings, Alan N., Engineering Services Group, Technology Applications,
Falls Church, Virginia

(Block 19 continued)

model-scale predictions. Three lift-fan designs are discussed and an increase in lift system efficiency of 10% to 15% is observed for a mixed-flow fan over a centrifugal-flow fan design.

Accession For	
NTIS GRA&I	<input checked="checked" type="checkbox"/>
DTIC TAB	<input type="checkbox"/>
Unannounced	<input type="checkbox"/>
Justification	
By	
Distribution/	
Availability Codes	
Dist	Avail and/or Special
A-1	



UNCLASSIFIED

SECURITY CLASSIFICATION OF THIS PAGE

TABLE OF CONTENTS

	Page
LIST OF FIGURES	111
NOTATION	1v
ABSTRACT	1
ADMINISTRATIVE INFORMATION	1
INTRODUCTION	1
DATA COLLECTION AND REDUCTION	5
EXPERIMENTAL RESULTS	6
LIFT FAN PERFORMANCE, P VERSUS Q	6
AIR DISTRIBUTION LOSSES	8
LIFT SYSTEM EFFICIENCY	11
CONCLUSIONS	14
REFERENCES	15

LIST OF FIGURES

1 - Pericell Skirt System with Lift Fan Arrangement	4
2 - Loop Fan and Cushion Fan Systems	4
3 - Performance Curves for the Three Lift Fans Examined	6
4 - Effect of Fan Room on Mixed Flow Fan C Performance	7
5 - Comparison of Nondimensional Fan Performance for Full-Scale Test Stand Results with Full-Scale Trial Results for Three Mixed Flow Fans C	8
6 - Pressure Loss from the Atmosphere to the Fan Room	9
7 - Pressure Loss from Diffuser Exit to the Loop and Cushion for Three Mixed Flow Fans C	10
8 - Variation of Feed Hole Coefficient with Loop Discharge	10
9 - Variation of Loop to Cushion Pressure Ratio with Lift System Flow Rate	11

	Page
10 - Comparison of Fan Total Efficiency for Full-Scale Test Stand Results with Full-Scale Trial Results for Three Mixed Flow Fans C	12
11 - Variation of Lift System Efficiency with Lift System Flow Rate--Data Correspond to 220 Feed Holes with Bow Seal Flaps Out	12
12 - Typical Distribution of Lift Power for Four N2 Settings	13

NOTATION

A	Area
$A_e = \pi b_2 d_2$	Fan exit area
b_2	Fan blade exit width
C_{FH}	Feed hole coefficient
CG	Center of gravity
C_L	Loss coefficient from diffuser exit to cushion
C_{L_1}	Loss coefficient
d_2	Fan diameter
HP	Lift system power
hp	Lift fan horsepower
L_B	Cushion beam
L_C	Cushion length
N	Lift fan rotational speed, rpm
%N2	Lift engine rotational speed, % of maximum lift engine power turbine rotational rate, 100% N2 = 15,400 rpm
P	Pressure
$P_C = W/L_B L_C$	Cushion pressure
P_L	Pressure loss
P_T	Lift fan to pressure at diffuser exit

Q	Flow rate, fan discharge
$u = \pi d_2 N / 60$	Fan lip speed
W	Craft weight
ΔP	Pressure drop
$\eta_{LS} = P_c Q / HP$	Lift system efficiency
$\eta_T = P_T Q / HP$	Fan diffuser exit total efficiency
ρ	Air mass density
$\phi = Q / A_e u$	Discharge coefficient
$\psi = P / \rho u^2$	Pressure coefficient

ABSTRACT

The design of a hovercraft lift system is normally based upon fairly simple hydraulic models of the lift system components. Lift system loss coefficients and fan efficiencies are determined from prior experience, empirical data bases and components or system model studies. The prediction of full-scale performance is complicated by the difficulty of establishing correspondence between model-scale and full-scale values of Reynolds number, Mach number and Euler number. Full-scale verification of the lift system design process is an essential part of hovercraft development.

This paper presents the results of a full-scale evaluation of the performance of a hovercraft lift system, and performance characteristics are compared with model-scale results. Comparisons of lift system loss coefficients show good correlation, but lift system efficiencies are shown to be significantly higher in full-scale results than from model-scale predictions. Three lift-fan designs are discussed and an increase in lift system efficiency of 10% to 15% is observed for a mixed-flow fan over a centrifugal-flow fan design. Reynolds number, Mach number, Lift fans, efficiency.

ADMINISTRATIVE INFORMATION

This study was sponsored by the Naval Sea Systems Command under Advanced Development Task Area S 1417, Task 14174 and administered by the Amphibious Assault Landing Craft Program Office and performed by the Special Ship and Ocean Systems Dynamics Branch (Code 1562) of the David W. Taylor Naval Ship Research and Development Center, Bethesda, Maryland.

INTRODUCTION

The design of a hovercraft lift system is normally based upon fairly simple hydraulic models with model-scale verification of lift system loss coefficients and system efficiencies. Full-scale evaluation of the lift system performance is a difficult and expensive procedure, but it is an essential part of the evolutionary design process since model-scale predictions are deficient in general respects. The correlation of model-scale and full-scale results suffers from the difficulty of equating three performance characteristics of the lift system. These are the Reynolds number, the Mach number and the Euler number.

The Reynolds number is defined as:

$$Rn = \frac{UD\rho}{\mu}$$

and represents the ratio of inertial to viscous forces in an hydraulic system. In general, equality of Reynolds numbers between model and full-scale systems insures that viscous phenomena such as separation and frictional drag are scaled. Viscous separation is the main characteristic linking the equalities of the lift system discharge coefficients. The Mach number

$$M = \frac{U}{c}$$

given as the ratio of flow to sonic velocity, represents the comparability of compression effects in model and full-scale lift systems. The Euler number

$$En = \frac{2P}{\rho U^2}$$

characterizes pressure losses which are energy dependent and represent effects which vary with atmospheric pressure. Low Mach number compressibility in the lift system is Euler dependent.

It is impossible to achieve model and full-scale equality for all three performance characteristics using air as a working fluid under conditions of normal atmospheric pressure. Individual lift system components can be (and routinely are) tested under equivalent conditions, but complete lift systems examined for intercomponent performance can only be fully and satisfactorily tested in full scale. This paper summarizes the results of a full-scale lift system evaluation through a presentation of data which were collected during a full-scale hovercraft lift system trial. Technical areas discussed in this document are lift system performance, skirts, and static cushionborne stability. The performance items

included are: lift fan pressure and flow; losses associated with the distribution of lift air through a pericell skirt system; cushionborne static pitch and roll stiffness; and the efficiency of lift system components. Comparisons of full-scale results with model-scale data or full-scale predictions are made where both data and predictions are available. The lift system of the hovercraft was evaluated with three different lift fan rotors. The original fan (Fan A) was a centrifugal flow compressor with a 4-ft (1.22-m) diameter and high-efficiency backward-airfoil blades. Predicted maximum total efficiency for this fan was 84 percent. A new lift fan rotor (Fan B) was designed and installed on the craft. This rotor was also a 4-ft (1.22-m) diameter centrifugal flow impeller but had a significantly reduced performance relative to the original fan. A mixed flow type of fan (Fan C) was chosen as the permanent lift fan for the vehicle. Both model-scale^{1*} and full-scale² performance tests were performed on the mixed flow design (Fan C). The performance of this design was sufficient to meet the pressure and flow rate characteristics given in Reference 3. Several skirt configurations were also examined during full-scale trials of the vehicle. Feed hole areas were changed to adjust the loop to cushion pressure ratio. Initial pitch and roll stiffnesses were found to be significantly less than that predicted from model experiments. Discrepancies were attributed, in part, to differences between model and full-scale skirt attachments. Several modifications to the skirts were made in order to increase the cushion stiffness; however, these modifications and their effects are not discussed in this document. A schematic of the loop-pericell skirt of the vehicle is shown in Figure 1. Lift fans 5 and 6 feed air directly into the cushion via ducts through the hull and are termed cushion fans. The remaining six fans are called loop fans (see Figure 2). The plenum area inside the craft superstructure in front of each fan is designated as the fan room. The pressure loss from the atmosphere to the fan room due to the air passing through the top opening in the superstructure will be discussed in another section of this document. The design conditions for the fans are for a lift system flow rate of 12,800 ft³/s (362.5 m³/s) and for standard atmospheric pressure on a 100°F day.

*A complete listing of references is given on page 15.

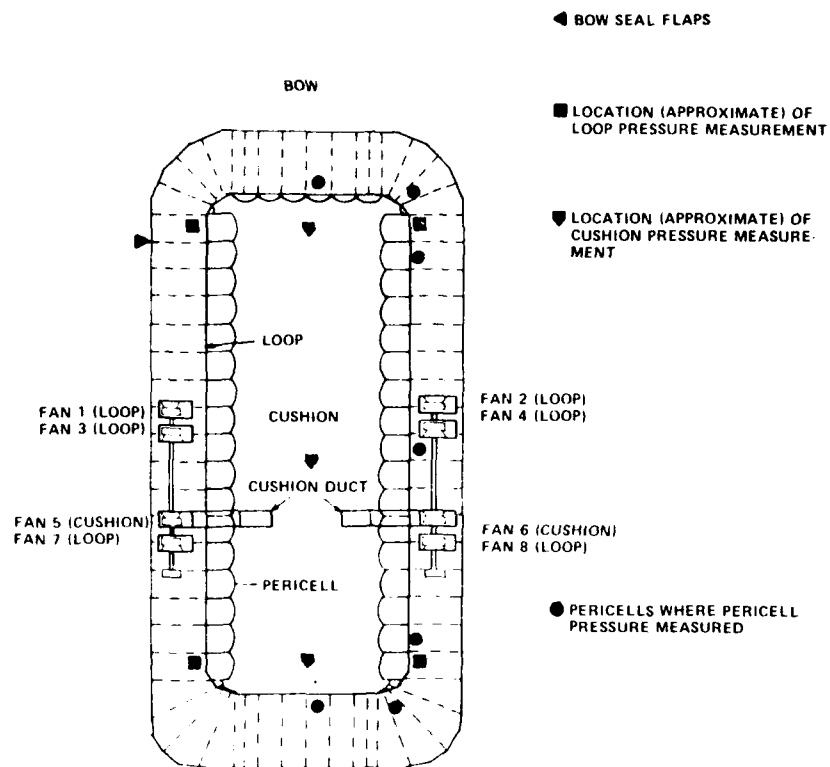


Figure 1 - Pericell Skirt System with Lift Fan Arrangement

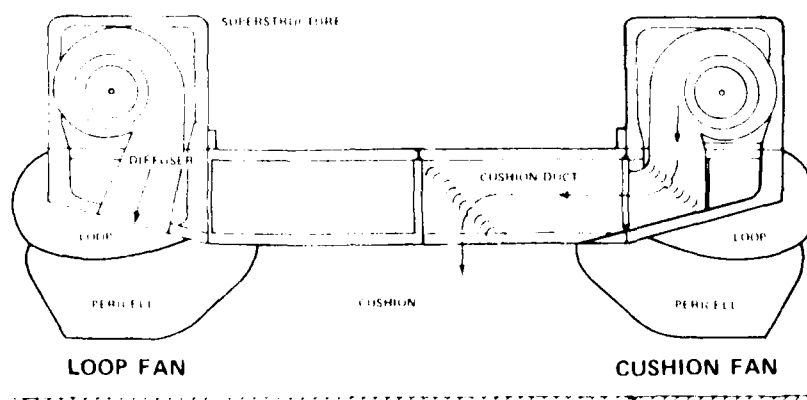


Figure 2 - Loop Fan and Cushion Fan Systems

DATA COLLECTION AND REDUCTION

The data presented in this document were obtained from quantities measured on the full-scale craft and from model and full-scale experiments. They include: fan room pressure; inlet bell pressure; loop, pericell and cushion pressure; fan torque and rpm; pitch and roll attitude; atmospheric pressure; temperature; and humidity. The approximate locations for loop, cushion, and pericell pressure measurements are shown in Figure 1. Fan torque and rpm were measured at the engine for the lift system. The four lift fans on each side of the JEFF (A) are on a common shaft and hence all fans on each side have the same rotational rate. It is assumed that each fan absorbs one quarter of the lift engine horsepower. Pitch and roll attitudes were measured with a stabilized gyro located near the craft CG. Atmospheric conditions were used to compute air density. It is assumed that the lift fans operated on the performance curve measured by Lorenc⁴ during a full-scale fan test. With this assumption and the flow rate measured with the inlet bell, the diffuser exit total pressure could be determined. Once this had been done, pressure losses were calculated from the diffuser exit to various places in the lift system. Losses were assumed to have the form

$$P_L = C_L \rho Q^2$$

where P_L = pressure loss

C_L = pressure loss coefficient

ρ = air mass density

Q = volumetric flow rate

An orifice coefficient was also calculated for the feed holes as shown below.

$$C_{FH} = \frac{Q}{A} \sqrt{\frac{\rho}{2\Delta P}}$$

where C_{FH} = feed hole coefficient

A = feed hole area

ΔP = pressure drop from loop to cushion

This was calculated using the lift fan discharge, Q , determined from the inlet bell calibration curve. A coefficient was calculated for each quadrant of the skirt.

EXPERIMENTAL RESULTS

LIFT FAN PERFORMANCE, P VERSUS Q

Figure 3 presents the nondimensional pressure versus flow performance curve for the three sets of lift fans that have been examined. The original Fan A and interim Fan B curves predicted full-scale performance based upon model tests as reported by Stek⁵ and Lavis,³ respectively. (The Reynolds' number scaling procedure applied to model data to produce the original and interim fan curves in Figure 3 is discussed by Moran and Jennings.⁶) The flow Fan C performance shown

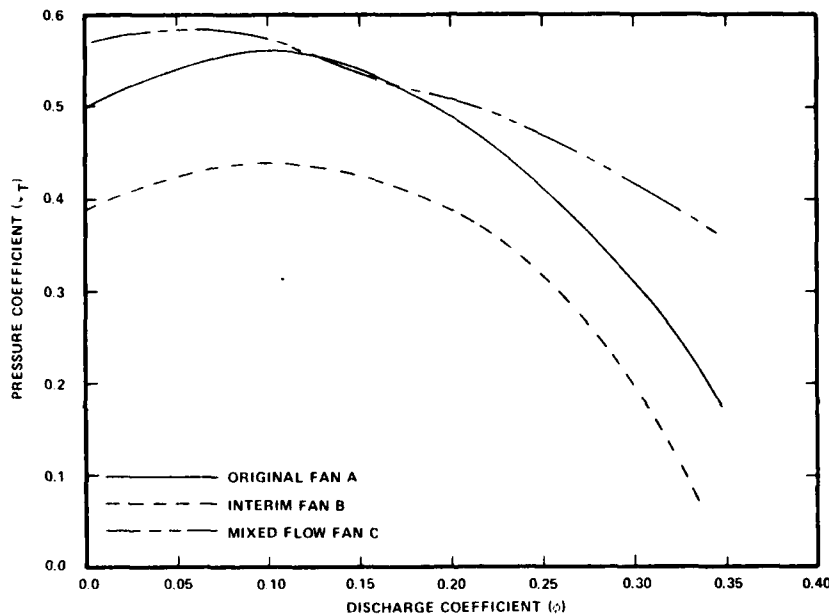


Figure 3 - Performance Curves for the Three Lift Fans Examined

is the full-scale data measured by Lorenc.⁴ Although the shape of the interim Fan B performance compares reasonably well with the performance of the mixed flow Fan C, its rotational speed limit of 2090 rpm and low efficiency precluded testing at high discharge pressures.

The effect of the fan room on mixed flow Fan C performance is shown in Figure 4. This result was reported by Lorenc⁴ in an experiment with a simulated fan room around a full-scale mixed flow fan. Significant degradation in performance is seen, particularly at higher discharge coefficients, ϕ , where the vehicle would normally operate. It was assumed for data reduction purposes in this document

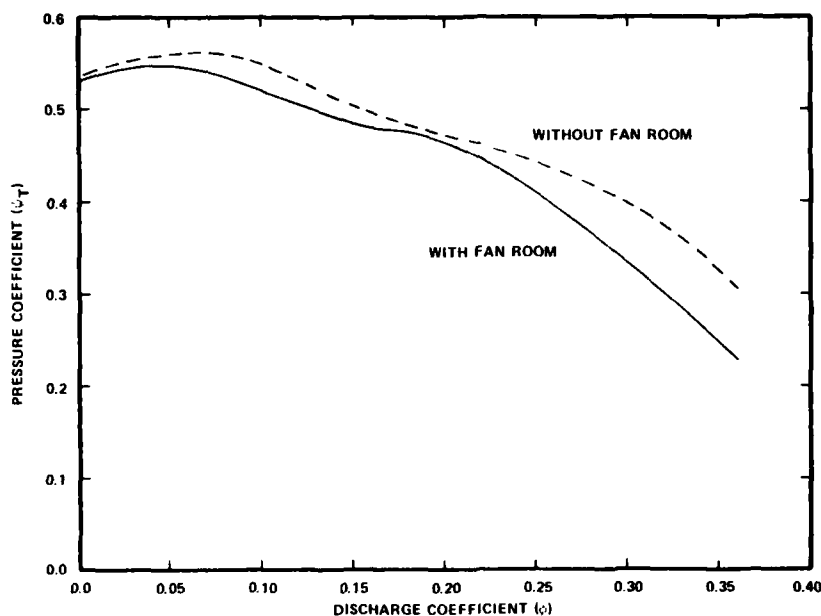


Figure 4 - Effect of Fan Room on Mixed Flow Fan C Performance

that the installed performance of the lift fans was represented by the curve of performance with the fan room. Figure 5 shows a comparison of data collected from full-scale trials with the fan performance curve from Figure 4 for three individual units on Fan C. The pressure loss from the diffuser exit to the loop for loop fans, and from the diffuser exit to the cushion for the cushion fan was determined by choosing the loss coefficient C_L such that the full-scale data would fit the fan performance curve. An average value of C_L was then taken for each lift fan. The values of C_L were determined to be 0.011, 0.0115, and 0.005 for lift Fans C4, C6 (cushion), and C8 (loop), respectively. It is seen, in other published data, that the cushion fan has a larger loss coefficient to the cushion than Fans C4 and C8 have to the loop. Lift Fan C8 also has a loss coefficient less than half that of the other fans. Typically, both loop and cushion pressure in the aft regions of the lift system were higher than those measured in the bow or along the sides, and contributed to a lower loss coefficient for Fan C8 than for Fan C4. Since the stern pericells are closed off, except for small drain holes, the flow through the aft section of the loop is smaller than that through the forward loop; losses have been assumed to be proportional to Q^2 and this reduces losses in the aft section.

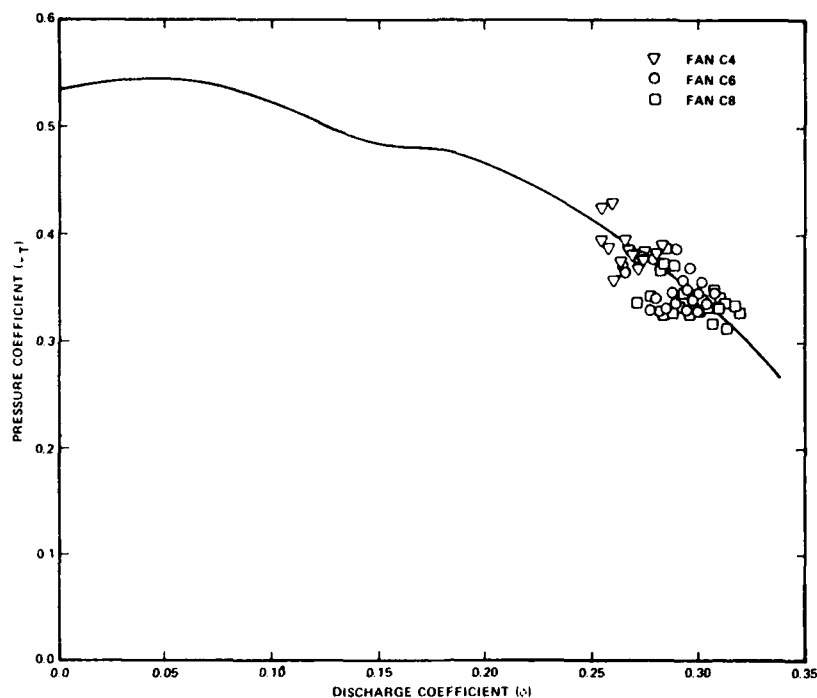


Figure 5 - Comparison of Nondimensional Fan Performance for Full-Scale Test Stand Results with Full-Scale Trial Results for Three Mixed Flow Fans C

AIR DISTRIBUTION LOSSES

The vehicle lift fans are housed within the craft superstructure, and a pressure loss is generated as lift air is drawn through the superstructure's openings. Figure 6 shows the loss curve for the fan room obtained from two of the full-scale fan tests. The large difference between the two full-scale trial curves may be attributed to the fact that the fan rooms are not all identical in geometry. Thus, local flows produce incorrect pressures for comparison purposes. Nonetheless, the loss curves for Fans C2 and C4 show a distinct similarity to the curve from the full-scale test. For data reduction purposes, the curve presented by Lorenc⁴ was used to determine fan room pressure losses. Also shown in Figure 6 is the pressure loss in the inlet bell reported by Lorenc.⁴ Total pressure loss in the inlet bell was found to be insignificant and was not accounted for in this presentation. Pressure loss curves from diffuser exit to the loop and from diffuser exit to the cushion

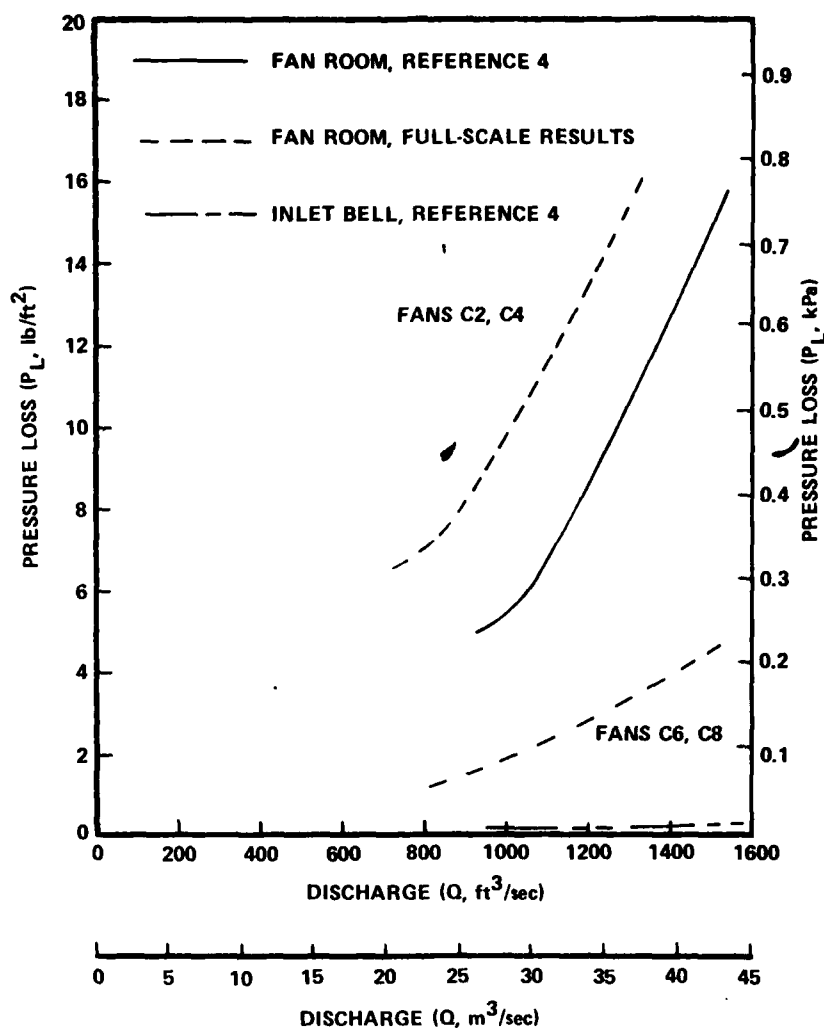


Figure 6 - Pressure Loss from the Atmosphere to the Fan Room

are shown in Figure 7 for Fans C4, C6, and C8. The loss curve from diffuser exit to loop was generated using the fitted loss coefficient, C_L . Similarly, the loss coefficient from the diffuser to the cushion, C_{L1} , was generated from the data points shown on the plots. The difference between these two curves represents the losses due to the feed holes and pericells. As noted for the loss coefficient, C_L , the diffuser to cushion loss, C_{L1} , for Fan C8 is less than C_{L1} for Fan C4. The variation of feed hole coefficient with loop flow rate is shown in Figure 8, where the coefficient C_{FH} is determined as previously defined. Full-scale results and

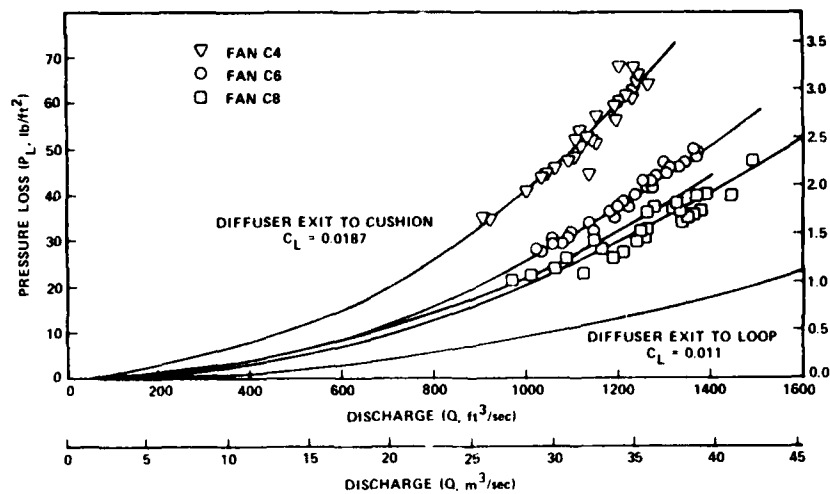


Figure 7 - Pressure Loss from Diffuser Exit to the Loop and Cushion for Three Mixed Flow Fans C

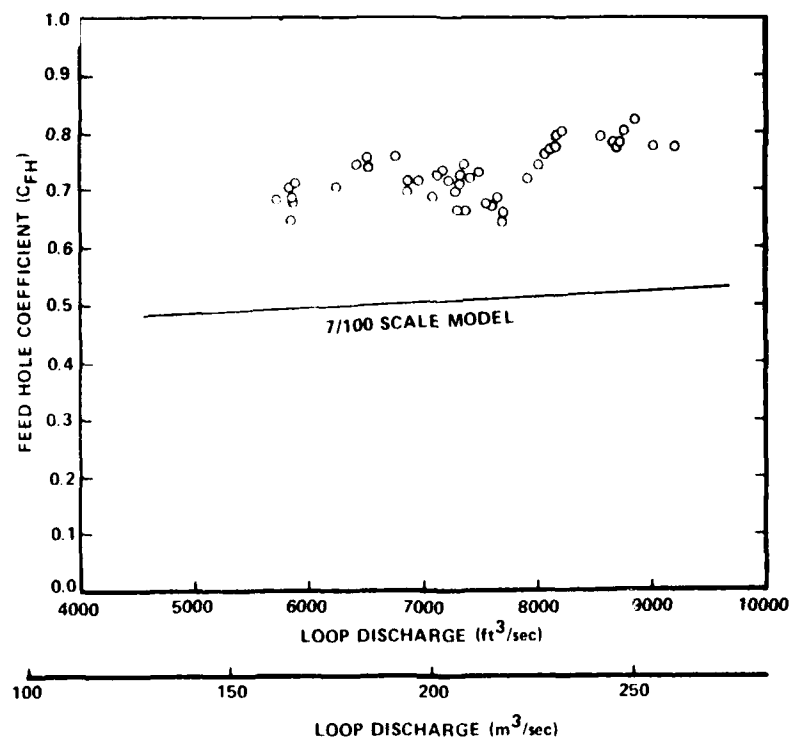


Figure 8 - Variation of Feed Hole Coefficient with Loop Discharge

those determined from a 7/100 hydrodynamic scale model of the vehicle reported by Jennings and Waters⁷ are shown. Unfortunately, the model lift system did not represent the full-scale vehicle exactly; resulting in the differences in C_{FH} shown. Figure 9 shows the variation of loop to cushion pressure ratio with lift system flow rate. All curves represent data taken with the interim B fans.⁸

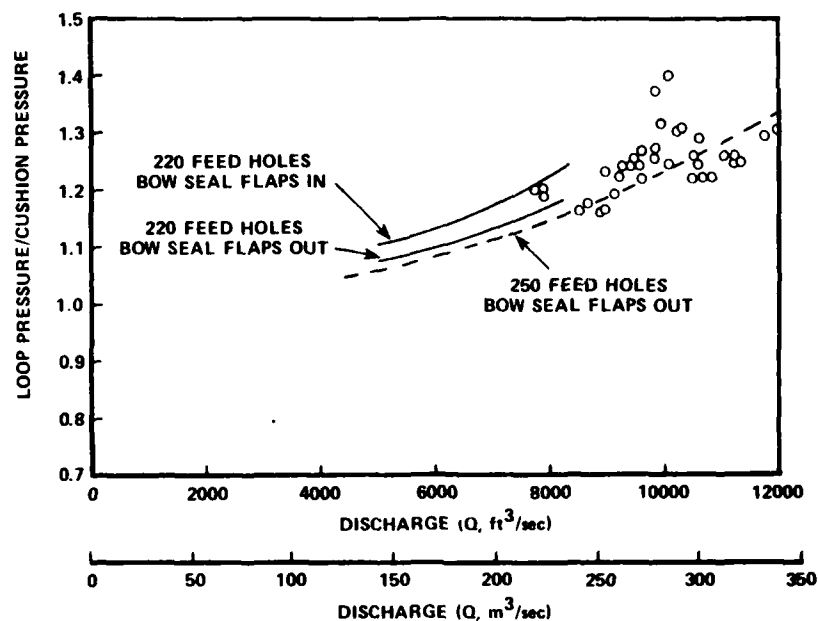


Figure 9 - Variation of Loop to Cushion Pressure Ratio with Lift System Flow Rate

LIFT SYSTEM EFFICIENCY

The variations of lift fan total efficiency, η_T , for Fans C4, C6, and C8 are shown in Figure 10. The curves are from Lorenc⁴ and the data points are from the full-scale trials.⁹ The variation of lift system efficiency, η_{LS} , with flow rate is shown in Figure 11. The curves labeled "Mods In" and "Mods Out" designate data from tests where the skirt configuration was being changed. Data obtained from the mixed flow C fans are indicated by points while data from the interim B fans are shown by the curves. The scatter in the data points makes it difficult to define a curve for η_{LS} with the mixed flow fans. Data at the same displacements tend to fall along a single curve, but the trends are not

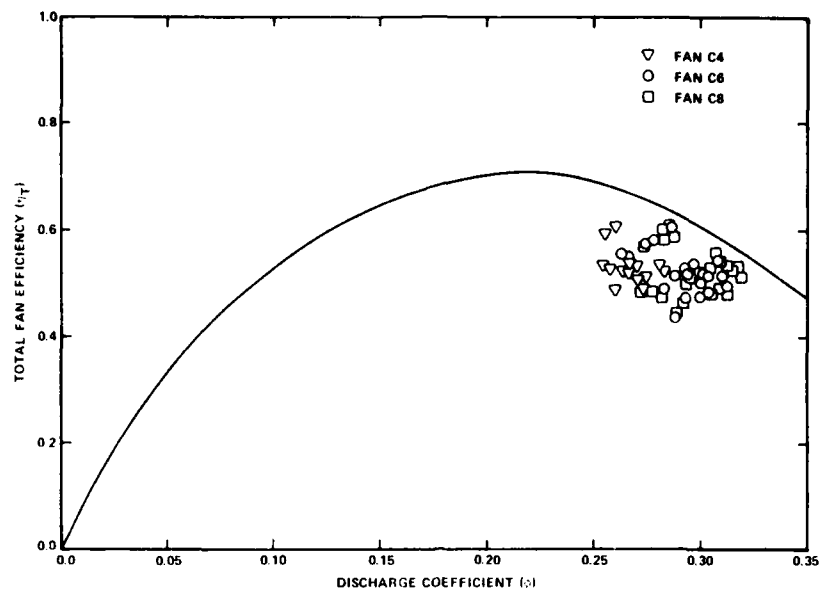


Figure 10 - Comparison of Fan Total Efficiency for Full-Scale Test Stand Results with Full-Scale Trial Results for Three Mixed Flow Fans C

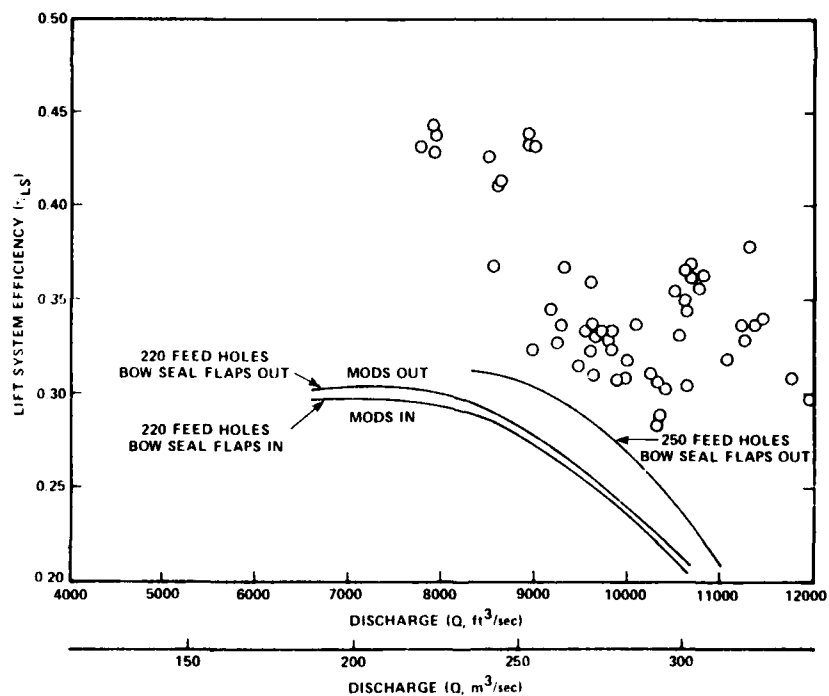


Figure 11 - Variation of Lift System Efficiency with Lift System Flow Rate--Data Correspond to 220 Feed Holes with Bow Seal Flaps Out

consistent among gross weights. Nevertheless, η_{LS} is larger with the mixed flow fans than with the interim fans. Lift system losses can be conveniently represented in graphs of the distribution of lift power as a function of lift engine rotational speed as shown in Figure 12. It is clear that the lift fan and diffuser power absorbed both tend to increase directly with the fan rotational speeds while the power used in going from the loop to the cushion (feed holes) remains fairly constant. The power absorbed by the cushion duct is included in the diffuser to loop portion. Similar presentations for fixed fan speed and varying cushion pressure show that the heavy displacement has a higher lift system efficiency than the lighter displacement. This result is true for all fan designs.

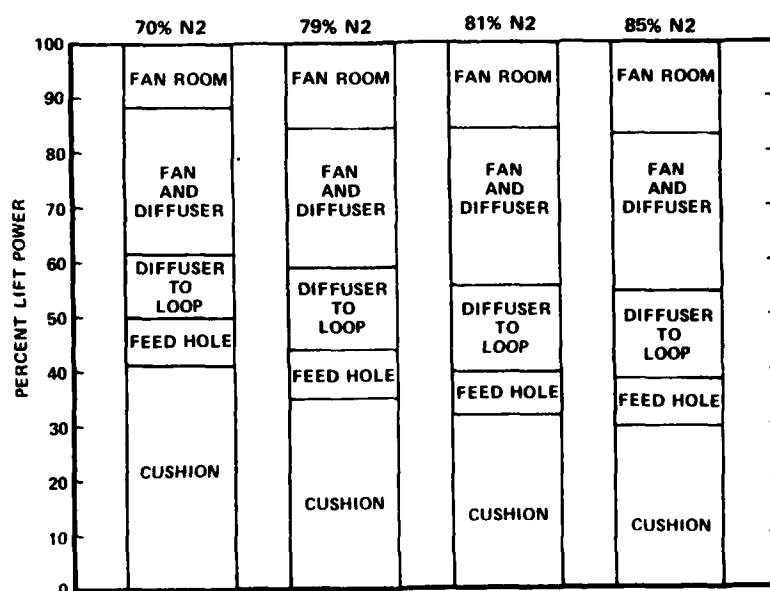


Figure 12 - Typical Distribution of Lift Power for Four N2 Settings

CONCLUSIONS

Full-scale and model-scale hovercraft lift system data have been presented and compared to demonstrate lift system performance variations for three lift fan systems. The following conclusions can be drawn from the results:

1. Significant losses are incurred due to the fan room. These losses consume 10% to 15% of total lift horsepower over a range of operating conditions.

2. Loss coefficients from diffuser exit to loop were determined to be 0.011 and 0.005 for Fans C4 and C8, respectively. The loss coefficient for the cushion duct was determined to be 0.0115. These losses would account for approximately 15% of total lift horsepower at the design condition with the mixed flow fans.

3. Pressure in the open pericells was found to be only slightly higher than cushion pressure for even trim conditions.

4. Lift fan total efficiency at the diffuser exit was found to be about 10 percentage points less than that predicted from the full-scale fan test.

5. Lift system efficiency was found to be 10 to 15 percentage points higher with the mixed flow fans than with the interim fans.

6. Lift system efficiency tended to decrease with increasing fan rotational speed and to increase with the gross weight.

REFERENCES

1. Lorenc, S.A., "Aerodynamic Design and Model Testing of JEFF (A) Mixed Flow Fan Rotor," Aerojet Liquid Rocket Co., Report 9752:0182 (Mar 1978).
2. Lorenc, S.A., "JEFF (A) Full Size Fan Testing," Aerojet Liquid Rocket Co., Report 9630:011 (Jun 1980).
3. Lavis, D.R. and A.W. Fowler, "The Summary Documentation of AALC Technology, Technology Batou A6.2, Lift Air Supply System," Band, Lavis and Associate, Inc. (Jan 1980).
4. Lorenc, S.A., "Advance Draft Copy Mixed Flow Fan Study," Aerojet Liquid Rocket Co., Report 2628:25 (Nov 1980).
5. Stek, J.B., "JEFF (A) Scale Model Test Program Lift Fan Performance Evaluations," Aerojet Liquid Rocket Co., Report 9737:0621 (Apr 1977).
6. Moran, D.D. and A.N. Jennings, "Lift Systems and Fan Performance of Air Cushion Supported Vehicles," DTNSRDC/SPD-0696-02 (Jul 1981).
7. Jennings, A.N. and R.T. Waters, "JEFF (A) 7/100 Scale Model Lift System Performance Characteristics," DTNSRDC/SPD-0850-01 (Jan 1980).
8. Aerojet General, "Investigation of Effect of Leakage Around Pericell Attachment Points of JEFF (A) Pitch and Roll Stiffness," Aerojet General Corporation (May 1978).
9. Jennings, A.N. and R.T. Waters, "LC JEFF (A) Lift System Full-Scale Trial Results," DTNSRDC/SPD-1012-0 (Nov 1983).

CENTER DISTRIBUTION

Copies	Code	Name
10	012.3	
1	122	
1	1221	
1	1222	
1	123	
1	1231	
1	156	
10	1562	
1	1603	
1	163	
1	2722	
10	5211.1	Reports Distribution
1	522.1	TIC LIB (C)
1	522.2	TIC LIB (A)

DTNSRDC ISSUES THREE TYPES OF REPORTS

1. DTNSRDC REPORTS, A FORMAL SERIES, CONTAIN INFORMATION OF PERMANENT TECHNICAL VALUE. THEY CARRY A CONSECUTIVE NUMERICAL IDENTIFICATION REGARDLESS OF THEIR CLASSIFICATION OR THE ORIGINATING DEPARTMENT.

2. DEPARTMENTAL REPORTS, A SEMIFORMAL SERIES, CONTAIN INFORMATION OF A PRELIMINARY, TEMPORARY, OR PROPRIETARY NATURE OR OF LIMITED INTEREST OR SIGNIFICANCE. THEY CARRY A DEPARTMENTAL ALPHANUMERICAL IDENTIFICATION.

3. TECHNICAL MEMORANDA, AN INFORMAL SERIES, CONTAIN TECHNICAL DOCUMENTATION OF LIMITED USE AND INTEREST. THEY ARE PRIMARILY WORKING PAPERS INTENDED FOR INTERNAL USE. THEY CARRY AN IDENTIFYING NUMBER WHICH INDICATES THEIR TYPE AND THE NUMERICAL CODE OF THE ORIGINATING DEPARTMENT. ANY DISTRIBUTION OUTSIDE DTNSRDC MUST BE APPROVED BY THE HEAD OF THE ORIGINATING DEPARTMENT ON A CASE-BY-CASE BASIS.

END

DTIC

6-86